# THERMAL CONDUCTIVITY OF NEUTRON-IRRADIATED SEMICONDUCTORS IN THE LOW-TEMPERATURE REGION

I. A. Gusev and A. F. Chudnovskii

Inzhenerno-Fizicheskii Zhurnal, Vol. 14, No. 6, pp. 1101–1116, 1968

UDC 536.21

The status of the question of the effect of fast-neutron irradiation on the thermal conductivity and structure of semiconductors is examined. It is shown that the reduction in thermal conductivity is the more considerable, the lower the temperature of investigation and the higher the fast-neutron integral flux, though not above a certain limit for a given material. Previously proposed models of the thermal conductivity of semiconductors for the temperature region 6–300° K are briefly examined. The question of the effect of annealing on the stability of neutron-induced defects in germanium and silicon is given separate consideration.

Modern semiconductor technology makes it possible to obtain perfect single crystals, i.e., crystals in which various types of lattice defects are reduced to a minimum. An enormous amount of work on the various properties of semiconductors points to the important part played by defects, particularly in connection with thermal conductivity. The study of the thermal conductivity of semiconductors irradiated with fast neutrons is of special importance, since neutron bombardment is a means of varying the number of defects. In particular, they can be made so numerous that the thermal conductivity of the crystalline specimen is sharply reduced. This effect is especially clearly expressed at low temperatures.

Apart from the considerable theoretical interest of the problem, it is also important from the practical standpoint of designing high-efficiency thermoelectric instruments. The performance of thermoelectric instruments is characterized by the figure of merit [1,2]:

$$Z = \frac{(Q_1 - Q_2)^2}{\left[\left(\frac{\chi_1}{\sigma_1}\right)^{\frac{1}{2}} + \left(\frac{\chi_2}{\sigma_2}\right)^{\frac{1}{2}}\right]^2}. \qquad (1)$$

Here, Q is the thermal emf; $\chi$ is the thermal conductivity; $\sigma$ is the electrical conductivity; and the subscripts 1 and 2 refer to the n- and p-type materials which form the contact. It is usual to employ p- and n-type semiconductors with similar values of the thermal and electrical conductivities and approximately equal thermal emf (of opposite sign). Under these conditions, it is possible to introduce the figure of merit for a single substance

$$Z = \frac{Q^2\sigma}{\chi}. \qquad (2)$$

Thus, finding materials for thermoelectric applications reduces to obtaining the maximum value of Z.

Since each of the quantities entering into Eq. (2) is a function of the physical, technological, and mechanical properties of the material, it is not possible to predict a priori the behavior of Z—special experiments are needed. Of course, it is desirable to study all the quantities Q, $\sigma$, and $\chi$ simultaneously.

Peierls [3] first drew attention to the specific behavior of the thermal conductivity at low temperatures, and Berman [4] demonstrated the effect of irradiation with fast neutrons on the thermal conductivity. The problem of studying the thermal conductivity under the simultaneous influence of the factors of temperature and neutron irradiation is a new one, and so far very little has been done in this direction. However, a number of authors have studied the thermal conductivity of semiconductors at low temperatures [5–13]. Many of the experimental data are explained by the models of Callaway [14, 15] and Klemens [16–18], which most closely reflect the actual transport processes.

Callaway assumes that all phonon-scattering processes can be represented by a relaxation time that is a function of frequency and temperature. He also assumes that the material is isotropically elastic and that scattering in the vibrational spectrum can be neglected. Moreover, he makes no distinction between longitudinal and transverse phonons.

Callaway considers the following scattering mechanisms: 1) impurity scattering, including point impurities (isotopes), whose relaxation time does not depend on temperature and is proportional to $\omega^{-4}$; 2) boundary scattering described by the constant relaxation time L/c, where c is the speed of sound and L is a certain length which is approximately equal in magnitude to the cross section of the specimen; 3) the normal three-phonon process, whose relaxation time is taken proportional to $(\omega^2T^3)^{-1}$, where $\omega$ is the angular frequency and T is the absolute temperature; 4) Umklapp processes, where the relaxation time is proportional to $[\exp(-\theta/aT)\omega^2T^3]^{-1}$, where $\theta$ is the Debye temperature and $a$ is a constant characterizing the vibrational spectrum of the material.

In solving the Boltzmann equation in the presence of a temperature gradient, Callaway introduces the relaxation times $\tau_N^{-1}$ and $\tau_U^{-1}$, which, respectively, characterize the N and U processes. Then, the combined relaxation time $\tau_C^{-1}$ is found to be

$$\tau_C^{-1} = \tau_N^{-1} + \tau_U^{-1}.$$

When $\tau_N$ is large, it is clear from Eqs. (12) and (16) of [14] that the thermal conductivity is essentially determined by the quantity $\tau_U^{-1}$, i.e., $\tau_C^{-1} = \tau_U^{-1}$. In expanded form, this can be written as follows:

$$\tau_U^{-1} = A\omega^4 + B_1 T^3 \omega^2 + \frac{c}{L} = \tau_C^{-1}. \quad (3)$$

The first term $A\omega^4$ reflects the process of scattering either at point impurities (isotopes) or at point defects, and A does not depend on temperature. The second term $B_1T^3\omega^2$ includes the Umklapp processes; $B_1$ contains the exponential temperature factor $\exp(-\theta/aT)$. The last term c/L describes the boundary scattering. A very interesting case is that in which the thermal conductivity measurements are made on an isotopically pure specimen, i.e., for $\tau_N^{-1} = B_2T^3\omega^2$, where $B_2$ does not depend on the temperature. Then, the combined relaxation time can be written in the following form:

$$\tau_C^{-1} = A\omega^4 + (B_1 + B_2)T^3\omega^2 + \frac{c}{L}. \quad (4)$$

According to Callaway, the thermal conductivity can be represented as

$$\chi = \frac{k}{2\pi c}(I_1 + \beta I_2), \quad (5)$$

where

$$I_1 = \int_0^{\frac{2\pi k\theta}{\hbar}} \tau_C \left(\frac{\hbar\omega}{2\pi kT}\right)^2 \frac{\exp\frac{\hbar\omega}{2\pi kT}}{\left[\exp\left(\frac{\hbar\omega}{2\pi kT}\right) - 1\right]^2} \omega^2 d\omega \quad (6)$$

and k is Boltzmann's constant.

Neglecting the second term (for simplicity) and substituting (6) into (5), we obtain

$$\chi = \frac{k}{2\pi c}\int_0^{\frac{2\pi k\theta}{\hbar}} \tau_C\left(\frac{\hbar\omega}{2\pi kT}\right) \times \frac{\exp\frac{\hbar\omega}{2\pi kT}}{\left[\exp\left(\frac{\hbar\omega}{2\pi kT}\right) - 1\right]^2} \omega^2 d\omega. \quad (7)$$

Introducing the dimensionless variable $x = \hbar\omega/2\pi kT$ and substituting (4) into (6), we have

$$I_1 = \left(\frac{2\pi kT}{\hbar}\right)\int_0^{\theta/T} \frac{x^4}{\left(Dx^4 + Ex^2 + \frac{c}{L}\right)} \frac{\exp x}{(\exp x - 1)^2} dx, \quad (8)$$

$$D = A\left(\frac{2\pi kT}{\hbar}\right)^4, \quad (9)$$

where

$$E = (B_1 + B_2)T^3\left(\frac{2\pi kT}{\hbar}\right)^2 \quad (10)$$

and h is Planck's constant.

At very low temperatures, D and E are much smaller than c/L, and the denominator can be simplified. The upper limit can be set equal to infinity, and in the first order of D and E we obtain

$$I_1 = \frac{4\pi}{15}\frac{L}{c}\left(\frac{2\pi kT}{\hbar}\right)^3 \times \left[1 - \frac{20\pi^2}{7}\frac{EL}{c} - 16\pi^4\frac{DL}{c}\right]; \quad (11)$$

i.e., in this case the thermal conductivity is proportional to $T^3$. If D is large, then the scattering at isotopes is very effective for short waves, and it is possible to evaluate (8) by assuming approximately that $x^2\exp x(\exp x - 1)^2$ is equal to unity. Thus, we have

$$I_1 = \frac{\pi}{2[A(B_1 + B_2)]^{1/2}T^{3/2}}\left[1 + \frac{2\left(\frac{cA}{L}\right)^{1/2}}{(B_1 + B_2)T^3}\right]^{-1/2}. \quad (12)$$

It has been shown that at temperatures above 30° K the correction in Eq. (12) is determined only by the first term when the brackets are removed. Then

$$I_1 = \frac{\pi}{2}\frac{1}{[A(B_1 + B_2)]^{1/2}T^{3/2}}\left[1 - \frac{\left(\frac{cA}{L}\right)^{1/2}}{(B_1 + B_2)T^3}\right]. \quad (13)$$

If we consider that in (5) the term $\beta I_2$ was neglected, and if it is in fact small, it follows from (13) that the thermal conductivity on both sides of the low-temperature maximum is proportional to $T^{3/2}$. If $B_2$ is only slightly less than $B_1$, an exponential dependence $\exp(\theta/2aT)$ is observed. Without presenting Callaway's calculation, in which he takes the term $\beta I_2$ into account, we obtain the expression for the thermal conductivity of an isotopically pure material in the following form:

$$\chi = \frac{2\pi k^2}{6h(B_1 + B_2)cT^2} \times \left\{1 - \pi^{\frac{3}{2}}\exp\left(-\frac{\theta}{T}\right)\left(\frac{\theta^2}{T^2} + \frac{2\theta}{T} + 2\right) - \frac{3h}{2\pi kT^{5/2}}\left[\frac{c}{L(B_1 + B_2)}\right] + \frac{7}{25}\frac{B_2}{B_1}\right\}, \quad (14)$$

and at very low temperatures

$$\chi = \frac{2k\pi^2 L}{15c^2}\left(\frac{2\pi kT}{\hbar}\right)^3\left[1 - 16A\left(\frac{2\pi^2 kT}{\hbar}\right)^4\frac{L}{c} - \frac{20}{7}B_1T^3\left(\frac{2\pi^2 kT}{\hbar}\right)^2\frac{L}{c}\right]. \quad (15)$$

It is clear from (15) that the normal processes do not make a contribution at very low temperatures (absence of $B_2$).

Although the Klemens model gives broader coverage to the possible phonon-scattering mechanisms and antedates the Callaway model, we have started by examining the Callaway model since it has been developed in exceptional detail. Apart from the processes considered above, the Klemens model also includes the high-order phonon-phonon interaction worked out by

Pomeranchuk [19]. However, since we are interested in low temperatures, basing ourselves on Pomeranchuk's research, we can state that in the given case these interactions play only a small part [20]. Klemens paid special attention to the effect of the isotopic composition of the crystal and explored the precise content of the coefficient A. It is clear from Eq. (4) that the first term can be written as $1/\tau = A\omega^4$ and, according to Klemens,

$$\frac{1}{\tau} = \left[\frac{V_0}{4\pi c^3}\sum_i f_i\left(1-\frac{m_i}{m}\right)^2\right]\omega^4 = \left[\frac{V_0}{4\pi c^3}\ \Gamma\right]\omega^4 = A\omega^4. \qquad (16)$$

For convenience, we introduce the following notation:

$$A = \frac{V_0}{4\pi c^3}\ \Gamma \qquad (17)$$

and

$$\Gamma = \sum f_i\left(1-\frac{m_i}{m}\right)^2, \qquad (18)$$

where $V_0$ is the atomic volume; $m_i$ is the mass of the i-th species of atom; m is the mean atomic mass; and $f_i$ is the percentage content of the atomic species $m_i$. In the case of a material containing one type of impurity

$$A = \frac{V_0}{4\pi c^3}\ n(1-n), \qquad (19)$$

where n is the impurity concentration.

It is now a matter of history that the first semiconductors to have their physical properties investigated were the monatomic semiconductors germanium and silicon. This was for both practical and theoretical reasons, since it is much easier to describe the processes in monatomic than in polyatomic semiconductors.

Experiments on the thermal conductivity of semiconductors irradiated with fast neutrons have shown that after irradiation various types of defects appear: a) point defects (vacancies, interstitials, and vacancy-interstitial pairs); b) group aggregations of vacancies and interstitials. Depending on the number and size of these defects and the isotopic composition of the specimens, the thermal conductivity of the semiconductors varies. On the other hand, it can be stated that the study of thermal conductivity, Hall mobility, electrical conductivity, thermal emf, and annealing in combination with the above-mentioned factors throws light on the nature and properties of "artificial" (induced) and natural defects.

Let us examine in more detail the experimental data obtained by studying the thermal conductivity of neutron-irradiated germanium and silicon.

## THERMAL CONDUCTIVITY OF GERMANIUM

**a) Temperature region from 80 to 300° K.** According to [18], for a nondegenerate semiconductor and low temperatures, the thermal resistance for phonons can be represented in the form

$$\frac{1}{\chi} = AT^{-3} + F(T) + BT^{-3}\exp\left(-\frac{\theta}{aT}\right), \qquad (20)$$

where A, B, and *a* are constants and $\theta$ is the Debye temperature. The first term represents boundary scattering. The second term characterizes phonon scattering at induced defects. In the case of point defects, F(T) is a linear function of temperature. The third term characterizes U-processes, which predominate at higher temperatures. The graphs in Fig. 1 represent the variation of the additional thermal resistance $1/\chi_{add}$ induced by bombardment in accordance with the relation

$$\frac{1}{\chi_{add}} = \frac{1}{\chi_a} - \frac{1}{\chi_0}, \qquad (21)$$

where $\chi_a$ and $\chi_0$ are, respectively, the actual and initial thermal conductivities. These quantities are represented graphically in Fig. 2, from which it is clear that the thermal conductivity decreases relative to the initial value the more considerably, the higher the neutron flux. The authors of [22] assumed that $\chi$ varies as a function of temperature, i.e., as $T^{-1.2}$, and this coincides with the data of [9–11]. For a dose of $6\cdot10^{17}$ n·cm$^{-2}$ (neutrons per square centimeter), $1/\chi_{add}$ diminishes markedly as the temperature rises. This may be attributable to phonon scattering at large defects. According to the theory [7], if phonons are scattered by this type of defect, the mean free path of the phonons does not depend on temperature, and the thermal resistance is inversely proportional to the specific heat; i.e., $1/\chi_{add}$ decreases as T increases.

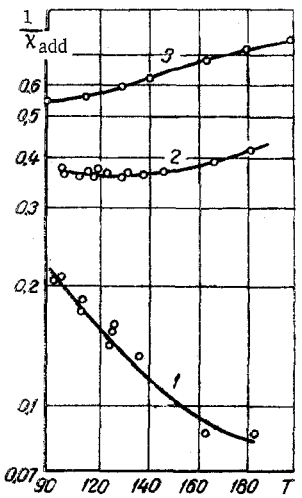


Fig. 1. Variation of additional thermal resistance $1/\chi_{add}$ (W$^{-1}$·deg$^{-1}$·cm) of germanium and silicon with temperature (°K): 1) and 2) germanium after irradiation at fluxes $\Phi$ = $= 6\cdot10^{17}$ n·cm$^{-2}$ and $1.2\cdot10^{18}$ n·cm$^{-2}$; 3) silicon after irradiation at $\Phi = 6\cdot10^{17}$ n·cm$^{-2}$.

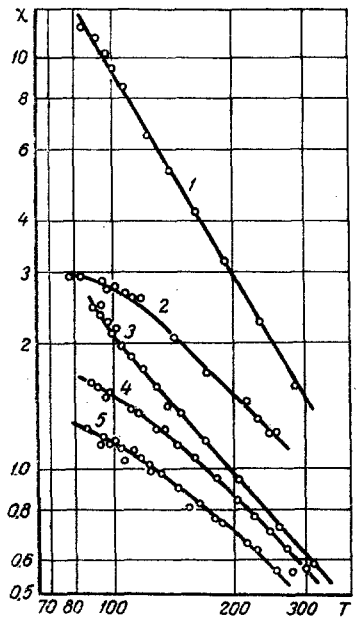


Fig. 2. Thermal conductivity χ (W · $deg^{-1} \cdot cm^{-1}$) of silicon (1, 2) and germanium (3, 4, 5): 1) before irradiation; 2) after irradiation at Φ = $= 1.2 \cdot 10^{18}$ n · $cm^{-2}$; 3) before irradiation; 4) and 5) after irradiation at Φ = $6 \cdot 10^{17}$ n · $cm^{-2}$ and $1.2 \cdot 10^{18}$ n · $cm^{-2}$.

For a dose of $1.2 \cdot 10^{18}$ n · $cm^{-2}$, the additional thermal resistance remains almost constant, increasing only slightly with increase in temperature. This is easily explained if it is assumed that large and relatively isolated defects are simultaneously induced during bombardment. If it is assumed that their contributions to the thermal resistance are supplementary, then $1/\chi_{add}$ must be regarded as being formed of two terms (only the left-hand side of Eq. (21) is considered), one of which varies in a direction opposite to the temperature, while the other varies in the same direction as the temperature. Very similar results were obtained in [21], where n-type germanium with a resistivity of 3 ohm · cm was investigated. The behavior of the corresponding curves (Fig. 1, curves 1, 2, and Fig. 2, curves 2, 3) is fundamentally the same. It appears that at low temperatures $1/\chi_{add}$ varies approximately as $T^{-2}$. This may hold true for doses not exceeding $6.7 \cdot 10^{17}$ n · $cm^{-2}$.

Using the Callaway model and the experimental data of [22], Albany and Vandervyver [23] demonstrated that the agreement between theory and experiment was quite good. Since the temperature region in question ranges from 80 to 300° K, in Eq. (5) it is necessary to take into account the term $\beta I_2$, where

$$I_2 = \int_0^{2\pi k\theta/h} \frac{\tau_C}{\tau_N} \left(\frac{h\omega}{2\pi T}\right)^2 \times \frac{\exp\left(\frac{h\omega}{2\pi kT}\right)}{\left[\exp\left(\frac{h\omega}{2\pi kT}\right) - 1\right]^2} \omega^2 d\omega; \qquad (22)$$

$$\beta = \int_0^{\theta/T} \frac{\tau_C}{\tau_N} \frac{\exp(x)\, x^4}{\exp x - 1} dx \Bigg/ \int_0^{\theta/T} \frac{1}{\tau_N} \left(1 - \frac{\tau_C}{\tau_N}\right) \frac{\exp(x)\, x^4}{[\exp(x) - 1]} dx. \qquad (23)$$

Expressions (22), (23) in conjunction with Eqs. (4)–(6) embrace four parameters (L, A, $B_1$, and $B_2$) that must be determined. The mean phonon velocity c and the Debye temperature for germanium [14] are estimated at $3.5 \cdot 10^5$ cm · $sec^{-1}$ and 375° K, respectively (it is assumed that their changes on irradiation can be neglected). In [8] it was shown that for unirradiated germanium L and A have the following values: 0.564 cm and $2.4 \cdot 10^{-44}$ $sec^3$. Above it was established [21, 22] that χ decreases as the flux increases, but, as the authors of [23] assume, this cannot be attributed exclusively to the increase $\tau^{-1} = A\omega^4$ in the scattering of phonons at point or "small" defects.

For unirradiated semiconductors,

$$L = 2\pi^{-1/2} S^{1/2}, \qquad (24)$$

where S is the cross section of the specimen, and A can be represented in the form

$$A = \frac{V_0}{4\pi c^3} \sum_i f_i \left(1 - \frac{m_i}{m}\right). \qquad (25)$$

Essentially, Eq. (25) is identical with Eq. (16). Albany and Vandervyver, using the experimental data of [22] and Eq. (5), determined the A and L for irradiated germanium by curve fitting (Table 1).

If it is assumed that the decrease in L is associated with the formation of defect aggregations and that the effective cross section for phonon scattering [24] is equal to the geometric cross section $\pi R^2$ of a sphere of radius R, the number of defect aggregations per $cm^3$ is given by the formula

$$N = \frac{1}{\pi R^2 L}. \qquad (26)$$

By means of the electron microscope we can determine both R and the surface density of the defect aggregations, and knowing the number of defects per unit length [25], we can find N and, hence, L. The values of $B_1 + B_2$ and $B_1/(B_1 + B_2)$ were taken from [14] and are equal to $2.8 \cdot 10^{-23}$ sec · $deg^{-3}$ and 0.07, respectively. The curves constructed from these data are in quite

Table 1

Values of the Parameters A and L for Unirradiated and Irradiated Germanium

| | Unirradiated Ge | Irradiated Ge | |
|---|---|---|---|
| | | $\Phi = 6 \cdot 10^{17}$ n · $cm^{-2}$ | $\Phi = 1.2 \cdot 10^{18}$ n · $cm^{-2}$ |
| $A \cdot 10^{44}$, $sec^3$ | 2.4 | 3.5 | 5 |
| L, cm | 0.564 | $6 \cdot 10^{-4}$ | $3.5 \cdot 10^{-4}$ |

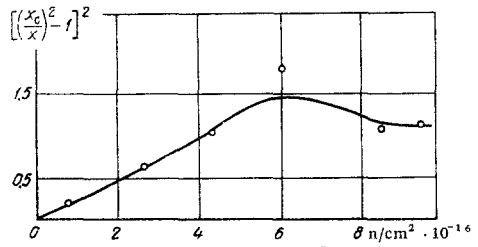


Fig. 3. Variation of $[(\chi_0/\chi)^2-1]^2$ during the irradiation of germanium with fast neutrons (T = 77° K, $\chi_0$ = 3 W · cm$^{-1}$ · deg$^{-1}$).

good agreement with the experimental points in Fig. 2 (curves 3, 4, 5).

In [26, 27] the change in the thermal conductivity of germanium (Fig. 3) during irradiation at 80° K was measured for the first time. This work is distinguished by the fact that the functions (which include the ratio of the initial to the measured thermal conductivity) have a different form. Here, the Callaway model is used as a basis for computing the dimensions of the defect aggregations. In particular, by using the experimental curve (Fig. 3), it is possible to construct the graph of thermal conductivity versus integral neutron flux.

**b) Temperature region below 80° K.** Dong [25, 28] measured the thermal conductivity of germanium with a resistivity of 10 ohm · cm by an absolute method up to 16° K. He also employed the Callaway model for computing the thermal conductivity. On the basis of the combined relaxation time (Eq. (4)), where B = $B_1 + B_2$, it is possible to obtain the following expression for the thermal conductivity of the system:

$$\chi = \frac{1}{2\pi^2 c}\int_0^{\omega_D} \frac{h^2\omega}{4\pi^2 kT\left(A\omega^4 + BT^3\omega^2 + \frac{c}{L}\right)} \times \times \frac{\exp\frac{h\omega}{2\pi kT}}{\left[\exp\frac{h\omega}{2\pi kT}-1\right]} d\omega, \qquad (27)$$

where $\omega_D = 2\pi k\theta/h = 4.9 \cdot 10^{13}$ rad/sec and $c = 3.5 \cdot 10^5$ cm/sec, $B = 2.8 \cdot 10^{-28}$ sec · deg$^{-3}$. Selecting the parameters A and L in Eq. (27) so that the calculated $\chi$ (curves 1, 2, and 3 in Fig. 4) coincides with the corresponding experimental points, one obtains (see Table 2) the numerical values of A and L.

As may be seen from Fig. 4 (curves 1, 2, 3), the agreement between theory and experiment is quite satisfactory. It is interesting to note that the factor A which, according to Klemens (Eq. (25)), is proportional to the number of point defects, varies only slightly, whereas L, which characterizes the mean free paths of the phonons, decreases considerably at low temperatures. It appears that here the effect of the isolated defects is masked by the isotopic defects, whose number in ordinary germanium is on the order of $10^{22}$ cm$^{-3}$. The sharp decrease in L is determined by the formation of a large number of regions of defect aggregation. In the given case ($\Phi = 5 \cdot 10^{17}$ n · cm$^{-2}$), the concentration of large defects reaches the order of $10^{16}$ cm$^{-3}$. It is assumed that the phonons are scattered uniformly at the isolated defects (in particular, isotopes) and partially at large defects. The mean free path of the phonons scattered at large defects is determined by relation (26):

$$\frac{1}{L} \leqslant \pi R^2 N.$$

Using Eq. (18) in the case of Frenkel defects (vacancy-interstitial), we can write relation (17) in the form

$$A = \frac{V_0^3}{4\pi c^3}\frac{n}{N}, \qquad (28)$$

where n is the defect density, and N is the atom density.

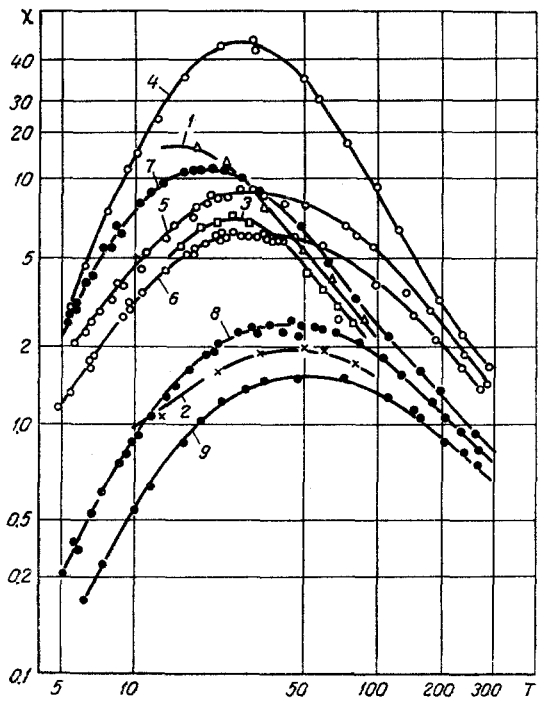


Fig. 4. Thermal conductivity $\chi$ (W · deg$^{-1}$ · cm$^{-1}$) of germanium (1, 2, 3—$\rho$ = 100 ohm · cm; 4, 5, 6—$\rho$ = 0.1 ohm · cm) and silicon (7, 8, 9—$\rho$ = 0.35 ohm · cm): 1) before irradiation; 2) after irradiation at $\Phi = 5 \cdot 10^{17}$ n · cm$^{-2}$; 3) after annealing at 100° C for 80 hr; 4) before irradiation; 5) and 6) after irradiation at $\Phi = 1.11 \cdot 10^{17}$ n · cm$^{-2}$ and $2.5 \cdot 10^{17}$ n · cm$^{-2}$; 7) before irradiation; 8) and 9) after irradiation at $\Phi = 1.11 \cdot 10^{17}$ n · cm$^{-2}$ and $2.5 \cdot 10^{17}$ n · cm$^{-2}$.

Table 2

Values of the Parameters A and L for Unirradiated and Irradiated Germanium

| Helium | A, sec$^3$ | L, cm |
|---|---|---|
| Before irradiation | $7 \cdot 10^{-44}$ | 0.5 |
| After irradiation $\Phi = 5 \cdot 10^{17}$ n · cm$^{-2}$ | $9 \cdot 10^{-44}$ | $10^{-3}$ |

However, the hypothesis of the formation of isolated defects is untenable. In fact, the concentration of vacancies and interstitials corresponding to a flux of $5 \cdot 10^{17}$ n · cm$^{-2}$ is on the order of $10^{18}$ cm$^{-3}$ and the value of A from relation (28) is less than its initial value. In Fig. 4 (curves 1, 2, and 3), it is clear that the thermal conductivity decreases sharply, especially at low temperatures. It is interesting to note that after irradiation the low-temperature maximum is shifted toward the region of higher temperatures. Exceptionally interesting, from the experimental standpoint, is the work of Albany and Vandervyver [29], who measured the thermal conductivity of n-type germanium on specimens with a resistivity of 0.1 ohm · cm by an absolute method in the region of 5° K. The germanium was irradiated with doses of $1.1 \cdot 10^{17}$ and $2.5 \cdot 10^{17}$ n · · cm$^{-2}$. After irradiation, the germanium was found to have been converted from the n-type to the p-type. The authors of [29] did not attempt a quantitative interpretation of these results in terms of any particular model. It should be noted that curves 4, 5, 6 (Fig. 4) have approximately the same shape as curves 1, 2, 3 (Fig. 4); i.e., as the dose increases the low-temperature maximum has a tendency to shift to the high-temperature region.

## THERMAL CONDUCTIVITY OF SILICON

**a) Temperature region from 80 to 300° K.** In [22], the thermal conductivity of silicon was determined at a dose of $1.2 \cdot 10^{18}$ n · cm$^{-2}$ (Fig. 2, curves 1 and 2). The additional thermal resistance is determined from relation (21) and is presented in Fig. 1 (curve 3). The picture is the same as for germanium irradiated under similar conditions and what was said in connection with germanium also applies here. However, in this case $\chi$ varies as a function of temperature in accordance with the law $T^{-1.6}$. The decrease in thermal conductivity is again attributed to the scattering of phonons at large and isolated defects.

Almost identical results were obtained by Albany and Vandervyver [30], who irradiated n-type silicon having a resistivity of 1 ohm · cm (Fig. 5, curves A to J). The Klemens model was used as a basis for interpretation. The thermal conductivity of the lattice for the combined relaxation time

$$\tau^{-1} = A\omega^4 + \frac{c}{L} \qquad (29)$$

can be expressed as

$$\chi_C = \frac{h}{4\pi^2 cAT}\left[\frac{1}{R}\int_0^1 \frac{x^4 \exp x}{(\exp x - 1)^2}\right] dx + \\ + \frac{1}{R}\int_1^\infty \frac{x^4 \exp x}{\left(1 + \frac{x^4}{R}\right)(\exp x - 1)^2}\, dx, \qquad (30)$$

where

$$R = \frac{c}{LA}\left(\frac{h}{2\pi kT}\right)^4. \qquad (31)$$

Numerical values of the second integral as a function of R are given in [24]. At high temperatures, it is necessary to take U-processes into account, and this can be expressed by the relation

$$\chi_U = BT^3 \exp\left(\frac{\theta}{aT}\right), \qquad (32)$$

where B and $a$ are equal to 8.25 W/cm · deg$^4$ and 1, respectively [6]. Thus, the thermal resistance is determined by three processes and, in accordance with the law of addition of thermal resistances, we have

$$W = \chi^{-1} = \chi_C^{-1} + \chi_U^{-1} = \\ = W_C + W_U. \qquad (33)$$

In Fig. 6 curves j and a represent the variation of the thermal resistance as a function of temperature (experimental values) before and after irradiation, respectively, while the curves j' and a' represent the difference $W_C = W_{exp} - W_U$ (squares). The quantity $W_C$ can be calculated from (30), where the values of A and L are selected so as to give the best agreement with

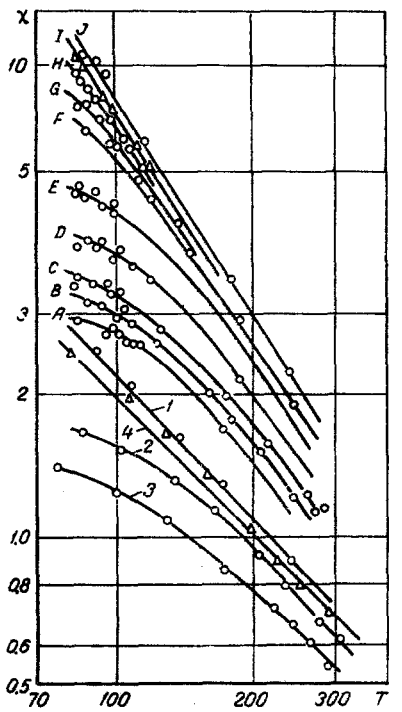


Fig. 5. Thermal conductivity $\chi$ (W · cm$^{-1}$ · · deg$^{-1}$) of germanium (curves 1, 2, 3, 4) and silicon (A, B, C, D, E, F, G, H, I, J, $\rho$ = = 1 ohm · cm): 1) before irradiation; 2 and 3) after irradiation at $\Phi = 6 \cdot 10^{17}$ and $1.2 \cdot \cdot 10^{18}$ n · cm$^{-2}$; 4) after annealing at 260° C for 2 hr; J) before irradiation; A) after irradiation at $\Phi = 1.2 \cdot 10^{18}$ n · cm$^{-2}$; B, C, D, E, F, G, H and I) after annealing for 1 hr at temperatures of 133, 166, 200, 233, 266, 300, 333, 366° C, respectively; I corresponds to additional annealing for 1 hr at 400° C.

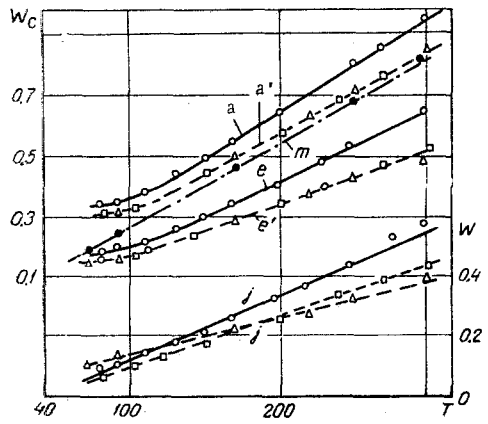

Fig. 6. Thermal resistance of silicon: j) unirradiated; a) irradiated; e) annealed; j', a', e') $W_C = W_{exp} - W_U$ (squares), $W_{calc}$ (triangles).

the experimental values of the thermal resistance on the temperature interval in question.

The calculated values of $W_C$ are represented by the triangles on curves j' and a', while the corresponding A and L are given in Table 3.

In Fig. 6 there is obviously good agreement (curve a') between the experimental data (squares) and the calculated values (triangles). The agreement is somewhat less satisfactory for the curve j'. With the object of stressing the importance of the factor L, taking for A the same values as for the irradiated silicon ($2.7 \cdot 10^{-44}$ sec$^3$) and for L the value for unirradiated silicon ($2.76 \cdot 10^{-1}$ cm), we find that the curve m thus calculated almost coincides with the curve a' (unirradiated silicon). At not very low temperatures, most of the longwave phonons obey the Debye distribution

$$\lambda = V_0^{\frac{1}{3}}\left(\frac{\theta}{T}\right), \qquad (34)$$

where $\lambda$ is the wavelength of the phonon. For temperatures of 80 and 300° K, $\lambda$ is 22 and 6 Å, respectively.

**b) Temperature region below 80° K.** The only measurements made so far have been on n-type silicon with a resistivity of 0.35 ohm · cm in the region of 5°K. Curves 7, 8, and 9 in Fig. 4 show the variation of the thermal conductivity as a function of neutron flux and temperature. From a comparison of curves 7, 8, 9 and 4, 5, 6 (Fig. 4), it is clear that, for identical temperatures and neutron fluxes, the thermal conductivity in the region at the left of the maximum is more sharply changed by irradiation in the case of germanium than in the case of silicon. There is practically no shift of the low-temperature maximum of the thermal conductivity of silicon to the high-temperature region with increase in temperature.

Table 3

Values of the Parameters A and L for Unirradiated and Irradiated Silicon

| Silicon | $A \cdot 10^{-44}$ sec$^3$ | $L \cdot 10^{3}$, cm$^{-1}$ |
|---|---|---|
| Irradiated | 2.7 | 1.5 |
| Unirradiated | 1.2 | 276 |

## STABILITY OF DEFECTS

**a) Germanium.** Since it has been established that, as a result of irradiation with fast neutrons, defects of various types are formed, it is important to investigate their stability. In [21] as the external factor it was decided to employ thermal heating of the irradiated specimen. Curve 4 in Fig. 5 characterizes the change in thermal conductivity as a result of a two-hour anneal at 260° C. The germanium specimen was irradiated with a dose of $6 \cdot 10^{17}$ n · cm$^{-2}$. This curve has a tendency to revert to the initial curve (before irradiation). The fact that this curve is parallel to the initial curve shows that the residual defects in the crystal are relatively isolated; i.e., it is primarily large aggregations that are affected. The authors of [21] state that the thermal conductivity is completely restored after annealing at 360° C for 2 hr. It should be noted that the crystal thus annealed is again converted into an n-type crystal. In relation to the elimination of large defect aggregations at sufficiently high temperatures (≥350° C), the latter assertion is consistent with the data of [31], where infrared absorption was used to study recovery processes. In another interesting experiment [25], neutron-irradiated germanium was annealed for 80 hr at 100° C in a vacuum. The thermal conductivity was restored almost to the initial value (Fig. 4, curve 3) in the temperature region from 50 to 100° K, but the recovery was weak at lower temperatures. Apparently the decisive role is played by the time and not the temperature factor (compare curve 4 in Fig. 5). It follows from Fig. 4 that there is a tendency for the low-temperature maximum of the thermal conductivity to be shifted to the low-temperature region. The quantity L, it appears, increases considerably, but does not reach the initial value, while the quantity A changes only slightly. These quantities have the following values: $3.5 \cdot 10^{-2}$ cm and $1.1 \cdot 10^{-43}$ sec$^3$, respectively (see Table 2). According to (26), the increase in L may be due to a decrease in the number or size of the aggregations, or to a simultaneous decrease in these two parameters. Since an increase is also accompanied by an increase in A, it may be assumed that a large number of aggregations are converted into small isolated defects (Eq. (26)).

**b) Silicon.** In [32], the effects of annealing silicon irradiated with an integral flux of $1.2 \cdot 10^{18}$ n · cm$^{-2}$ were studied in the temperature region from 70 to 400°C. The thermal resistance was used to characterize the changes taking place in the material. Assuming that the increase in resistance is proportional to the defect density, we can determine the fraction of unannealed defects

$$f = \frac{W - W_i}{W_a - W_i} \qquad (35)$$

for the temperature interval in question. Here, W is the thermal resistance before irradiation; $W_a$ is the thermal resistance after irradiation, but before annealing; and $W_i$ is the thermal resistance after irradiation and annealing. The rate of change of the number of defects with temperature can be written in the form

$$\frac{dn}{dT} = -\frac{\nu}{v} n\gamma \exp\left(-\frac{E}{kT}\right), \qquad (36)$$

where $\nu$ is the frequency factor; n is the defect density; $\gamma$ is a constant of kinetic order; E is the activation energy of the recovery processes; k is Boltzmann's constant; and T is the absolute temperature. Since a relation of proportionality exists between n and $f$, for the point of inflection we have

$$\frac{\gamma}{f}\frac{df}{dT} = -\frac{E}{kT^2}.$$

For $\gamma = 2$ the activation energy is $1.0 \pm 0.1$ eV. The same value of the activation energy (1.09 eV) was obtained by Mayer and Lécomte [33]. Above we saw that large defects recover first, and only then the point defects. The authors show that a similar process takes place in this case also, namely, at 233° C, 73% of the residual unannealed defects correspond to point defects. At higher temperatures (from 400 to 1100° C), it is exclusively a question of radiation-induced point defects. Only a fraction of the point defects, estimated at 8%, remains unannealed. Extensive research into the effect of annealing on thermal conductivity is reported in [30]. Irradiated silicon (integral flux $1.2 \cdot 10^{18}$ $n \cdot cm^{-2}$, curve A, Fig. 5) was subjected to successive isochronous anneals lasting 1 hr in each case. The intermediate curves (B, C, D, E, F, G, and H, Fig. 5) were recorded at temperatures of 133, 166, 200, 233, 266, 300 and 333° C. Curve 1 was recorded at 366° C. Annealing was carried out for 1 hr plus an additional hour at 400° C (no practical difference was noted between these anneals). It is quite clear from the figure that as the annealing temperature increases so does the thermal conductivity (the number of phonon-scattering defects is reduced), and at 400° C it almost reaches its original value.

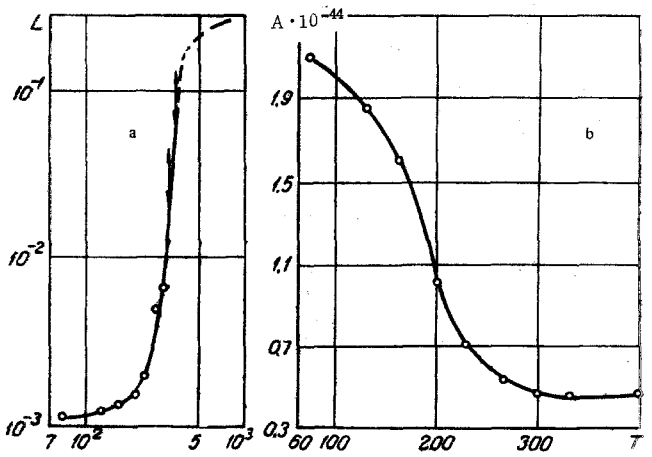

Fig. 7. Variation of the parameters L ($\tau^{-1} = c/L$) (a) and A ($\tau^{-1} = A\omega^4$) (b) as a function of annealing temperature (°C).

In addition to their study of the effect of annealing on thermal conductivity [30], in [34] Albany and Vandervyver studied the question of the variation of the parameters L and A. The variation of L and A as functions of temperature is shown in Fig. 7. It is clear from Fig. 7a that L begins to decrease particularly sharply at a temperature of about 350–300° C. If it is assumed that the number of defects, given by Eq. (26), does not decrease, it follows that their size decreases. This is confirmed by the behavior of the quantity A (Fig. 7b), especially in the temperature region above 300° C. But, in reality, the decrease in the size of the defects is accompanied by their reduction.

## SUMMARY

1. Irradiation with fast neutrons reduces the thermal conductivity of germanium and silicon semiconductors. The reduction is the greater, the higher the temperature, and the higher the integral neutron flux, though not beyond a certain limit for a given material.
2. The sharp decrease in the quantity L, characterizing the mean free path of the phonon after irradiation with fast neutrons, is a result of the formation of a large number of regions of defect aggregation.
3. For germanium and silicon in the temperature range from 80 to 300° K the thermal conductivity varies as a function of temperature as $T^{-1.2}$ and $T^{-1.6}$, respectively.
4. With increase in the integral neutron flux through single-crystal germanium, the low-temperature maximum of its thermal conductivity has a tendency to shift to the region of higher temperatures; in the case of silicon, the low-temperature maximum is not displaced.
5. In the temperature range from 5 to 20° K, the change in the thermal conductivity of germanium after irradiation is greater by a factor of 2–3 than the change in the thermal conductivity of silicon.
6. At annealing temperatures of 350° C, the thermal conductivity of neutron-irradiated germanium and silicon is almost completely restored to the original value.
7. It follows from the experimental data that the regions of defect aggregation are 50–150 Å in size.

## NOTATION

Z is a figure of merit; Q is the thermal emf; $\chi$ is the thermal conductivity; $\sigma$ is the electrical conductivity; $\omega$ is the angular frequency; c is the velocity of light; T is the absolute temperature in °K; $\theta$ is the Debye temperature; $\tau_N^{-1}$ is the relaxation time for normal processes; $\tau_U^{-1}$ is the relaxation time for Umklapp processes; k is Boltzmann's constant; $B_1$ and $B_2$ are proportionality factors; $V_0$ is the atomic volume, q is the electronic charge; $\Phi$ is the fast-neutron integral flux.

REFERENCES


1. J. R. Drabble and H. J. Goldsmid, Thermal Conduction in Semiconductors [Russian translation], IL, 1963.

2. A. F. Ioffe, Semiconductor Thermoelements [in Russian], Izd-vo AN SSSR, 1960.

3. R. E. Peierls, Ann. d. Phys., **3**, 1055, 1929.

4. R. Berman, Proc. Roy. Soc., A**208**, 90, 1951.

5. P. Carruthers, Rev. Mod. Phys., **33**, 92, 1961.

6. B. K. Agrawal and G. S. Verma, Phys. Rev., **126**, 24, 1962.

7. J. P. Ziman, Electrons and Phonons, 1960.

8. A. M. Toxen, Phys. Rev., **122**, 450, 1961.

9. G. A. Slack and C. Glassbrenner, Phys. Rev., **120**, 782, 1960.

10. T. N. Geballe and G. W. Hull, Phys. Rev., **110**, 773, 1958.

11. I. A. Carruthers, T. N. Geballe, et al., Proc. Roy. Soc., A**238**, 502, 1957.

12. R. W. Keyes, Phys. Rev., **122**, 1171, 1961.

13. J. F. Gott and N. Pearlman, 7th Intern. Conf. on Low Temperature Phys., Toronto, 1960.

14. J. Callaway, Phys. Rev., **113**, 1046, 1959.

15. J. Callaway and H. Bayer, Phys. Rev., **120**, 1149, 1960.

16. P. G. Klemens, Proc. Roy. Soc., A**208**, 108, 1951.

17. P. G. Klemens, Proc. Phys. Soc., A**68**, 1113, 1955.

18. P. G. Klemens, Solid State Phys., **7**, 1, 1958.

19. I. Pomeranchuk, Fizika, **4**, 357, 1941.

20. I. Pomeranchuk, Fizika, **6**, 237, 1942.

21. N. V. Dong and P. N. Tung, J. Electron, and Control, **15**, 547, 1963.

22. N. V. Dong et al., J. Phys., **24**, 464, 1963.

23. H. S. Albany and M. Vandervyver, J. Phys., **25**, 978, 1964.

24. G. Slack, Phys. Rev., **105**, 832, 1957.

25. N. V. Dong, J. Phys., **27**, 128, 1966.

26. N. V. Dong, J. Appl. Phys., **36**, 3450, 1965.

27. N. V. Dong, C. R. Acad. Sci., **260**, 5512, 1965.

28. N. V. Dong, C. R. Acad. Sci., **259**, 1091, 1964.

29. M. Vandervyver and H. S. Albany, Phys. Letters, **19**, 376, 1965.

30. H. S. Albany and M. Vandervyver, C. R. Acad. Sci., **257**, 859, 1963.

31. R. E. Whan, J. Appl. Phys., **37**, 2435, 1966.

32. M. Vandervyver and H. S. Albany, C. R. Acad. Sci., **257**, 1252, 1963.

33. G. Mayer and M. Lécomte, Phys. Rad., **21**, 242, 1960.

34. H. S. Albany and M. Vandervyver, 7th Congress Intern. Phys. Semiconduct., Paris-Rayanmont, 1964, vol. 3, Paris, 1965.



Agrophysics Institute,
Leningrad